Analyses of unintentional intensity modulation in all-fiber acousto-optic tunable filters

Kwang Jo Lee,[1, 3, 4,*] In-Kag Hwang,[1] Hyun Chul Park,[2] Ki Hak Nam,[3] and Byoung Yoon Kim[3]

[1]*Department of Physics, Chonnam National University, 300 Yongbong-dong, Buk-gu, Gwangju, 500-757, Korea*
[2]*Instrumentation & Control Research Group, POSLAB, 1, Goedong-dong, Nam-gu, Pohang, Gyeongbuk, 790-300, Korea*
[3]*Department of Physics, Korea Advanced Institute of Science and Technology, 373-1 Guseong-dong, Yuseong-gu, Daejeon, 305-701, Korea*
[4]*Currently with the Optoelectronics Research Centre, University of Southampton, Southampton, SO17 1BJ, UK*
** kjl@kaist.ac.kr*

Abstract: We theoretically and experimentally analyze unintentional intensity modulation phenomena in two types of all-fiber acousto-optic tunable filters utilizing flexural and torsional acoustic waves. Output filter signal at a resonant wavelength shows time-varying oscillations with even- and odd-order harmonics of applied acoustic frequency, which are explained by two factors of static mode coupling and acoustic back reflection. The magnitudes of static coupling and acoustic reflection in our devices are estimated from the measured first and second harmonic modulation powers.

OCIS codes: (060.2310) Fiber optics; (230.1040) Acousto-optical devices.

References and links

1. D. Sadot, and E. Boimovich, "Tunable optical filters for dense WDM networks," IEEE Commun. Mag. **36**(12), 50–55 (1998).
2. H. S. Kim, S. H. Yun, I. K. Kwang, and B. Y. Kim, "All-fiber acousto-optic tunable notch filter with electronically controllable spectral profile," Opt. Lett. **22**(19), 1476–1478 (1997).
3. K. J. Lee, D.-I. Yeom, and B. Y. Kim, "Narrowband, polarization insensitive all-fiber acousto-optic tunable bandpass filter," Opt. Express **15**(6), 2987–2992 (2007).
4. M. Berwick, C. N. Pannell, P. St. J. Russell, and D. A. Jackson, "Demonstration of birefringent optical fibre frequency shifter employing torsional acoustic waves," Electron. Lett. **27**(9), 713–715 (1991).
5. K. J. Lee, H. C. Park, and B. Y. Kim, "Highly efficient all-fiber tunable polarization filter using torsional acoustic wave," Opt. Express **15**(19), 12362–12367 (2007).
6. H. E. Engan, "Analysis of polarization-mode coupling by acoustic torsional waves in optical fibers," J. Opt. Soc. Am. A **13**(1), 112–118 (1996).
7. H. E. Engan, D. Östling, P. O. Kval, and J. O. Askautrud, "Wideband operation of horns for excitation of acoustic modes in optical fibers," Proc. SPIE **2360**, 568–571 (1994).
8. S. S. Lee, H. S. Kim, I. K. Hwang, and S. H. Yun, "Highly-efficient broadband acoustic transducer for all-fiber acousto-optic devices," Electron. Lett. **39**(18), 1309–1310 (2003).
9. Q. Li, A. A. Au, C.-H. Lin, I. V. Tomov, and H. P. Lee, "Performance characteristics of a WDM channel monitor based on an all-fiber AOTF with an on-fiber photodetector," IEEE Photon. Technol. Lett. **15**(5), 718–720 (2003).
10. J. Zhao, X. Liu, Y. Wang, and Y. Luo, "Bending effect on fiber acousto-optic mode coupling," Appl. Opt. **44**(24), 5101–5104 (2005).
11. H. C. Park, B. Y. Kim, and H. S. Park, "Apodization of elliptical-core two-mode fiber acousto-optic filter based on acoustic polarization control," Opt. Lett. **30**(23), 3126–3128 (2005).
12. A. Diez, G. Kakarantzas, T. A. Birks, and P. St. J. Russell, "High strain-induced wavelength tunability in tapered fibre acousto-optic filters," Electron. Lett. **36**(14), 1187–1188 (2000).
13. K. J. Lee, I.-K. Hwang, H. C. Park, and B. Y. Kim, "Axial strain dependence of all-fiber acousto-optic tunable filters," Opt. Express **17**(4), 2348–2357 (2009).
14. W. V. Sorin, "Methods and apparatus for measuring the power spectrum of optical signals," US Patent 6801686 (2004).
15. A. A. Au, Q. Li, C.-H. Lin, and H. P. Lee, "Effects of acoustic reflection on the performance of a cladding-etched all-fiber acoustooptic variable optical attenuator," IEEE Photon. Technol. Lett. **16**(1), 150–152 (2004).
16. B. Y. Kim, J. N. Blake, H. E. Engan, and H. J. Shaw, "All-fiber acousto-optic frequency shifter," Opt. Lett. **11**(6), 389–391 (1986).

#120153 - $15.00 USD Received 18 Nov 2009; revised 30 Jan 2010; accepted 2 Feb 2010; published 16 Feb 2010

1. Introduction

Various types of tunable optical filters such as Fabry Perot interferometer, fiber Bragg grating, electro-optical tunable filter, and ring resonator tunable filter are in common use in optical communication and sensor systems [1]. In particular, all-fiber acousto-optic tunable filters (AOTFs) have attracted considerable interest because of their advantages such as low insertion loss, wide and fast wavelength tuning, low polarization dependence, and variable attenuation via simple electronic control [2–5]. The all-fiber AOTFs have been demonstrated based on wavelength selective acousto-optic (AO) mode coupling by traveling flexural [2, 3] or torsional acoustic wave [4–6]. In these devices, the acoustic waves produce the resonant coupling between two spatial modes in an optical fiber (for flexural wave) or between two polarization modes in a highly birefringent (HB) fiber (for torsional wave). As well as the demonstration of the device principle, the efficient acoustic transducer designs [7, 8] and the effects of various perturbations including temperature fluctuation [9], fiber bending [10], twist [11], and axial strain [12,13] have been reported previously. Suppression of unintentional intensity modulation in output filter signal is also a critical factor in practical application of the devices. In wavelength-division multiplexing (WDM) communication, the temporal intensity fluctuation larger than 3% at 10-dB attenuation level significantly deteriorates the signal quality [14]. It has been also reported that the maximum attenuation of all-fiber AOTF utilizing flexural acoustic wave can be reduced due to the presence of intensity modulation [15]. Ref [15]. described the acoustic back reflection in AO interaction region induced the modulation at even-order harmonics of applied acoustic frequency. However, in experiments it is observed that output filter signal at resonant peak shows time-varying oscillation with both even- and odd-order harmonics of applied acoustic frequency. The origin of these harmonics in intensity modulation has not been fully explained to date.

In this paper, we theoretically and experimentally analyze the intensity modulation phenomena in two types of all-fiber AOTFs utilizing flexural and torsional acoustic waves. We will explain the origins of various harmonic modulations in connection with static mode coupling and acoustic back reflection. The amplitude of each harmonic modulation will be derived using our theoretical model, and the magnitudes of static coupling and acoustic back reflection will be deduced from the measured modulation amplitudes.

2. Analyses of unintentional intensity modulation in two types of all-fiber AOTFs

Figure 1 shows the schematics of experimental setups used to measure the time-dependent intensity modulation in the all-fiber flexural mode AOTF [Fig. 1(a)] and torsional mode AOTF [Fig. 1(b)]. The device in Fig. 1(a) is composed of an acoustic transducer, a standard single mode fiber (SMF), and an acoustic damper. The acoustic transducer comprises a glass horn and a lead zirconate titanate (PZT) plate attached to wider end of the horn. The flexural acoustic wave generated by the coaxial acoustic transducer propagates along a bare section of the fiber bonded to the central hole in the horn and is absorbed by the acoustic damper at the end of the AO interaction region. The periodic micro-bends in the fiber induced by the flexural acoustic wave perturb the incident LP_{01} mode in the core and causes coupling to the anti-symmetric LP_{11} mode in the cladding at resonant wavelength where the phase matching condition is satisfied [13]. The coupled LP_{11} mode is completely scattered or absorbed by the polymer jacket on the fiber before entering the optical detector, resulting in a wavelength notch in the transmission spectrum. The configuration of the device in Fig. 1(b) is very similar to that of Fig. 1(a), but it uses a HB fiber and two polarizers at input and output. The acoustic transducer to generate a torsional wave is composed of two pieces of PZT half-discs with opposite polling directions [5]. When a radio frequency (RF) electric signal is applied, they oscillate in opposite direction to effectively twist the horn. The torsional acoustic wave perturbs the input (horizontal) polarization of the LP_{01} mode and cause the energy transfer to orthogonal (vertical) polarization of the LP_{01} mode at the resonant wavelength. Then only the coupled light is selected by the output vertical polarizer, resulting in bandpass filtering. The

#120153 - $15.00 USD Received 18 Nov 2009; revised 30 Jan 2010; accepted 2 Feb 2010; published 16 Feb 2010

inset of Fig. 1(b) shows the cross-section of the HB fiber with elliptical stress member used in this experiment.

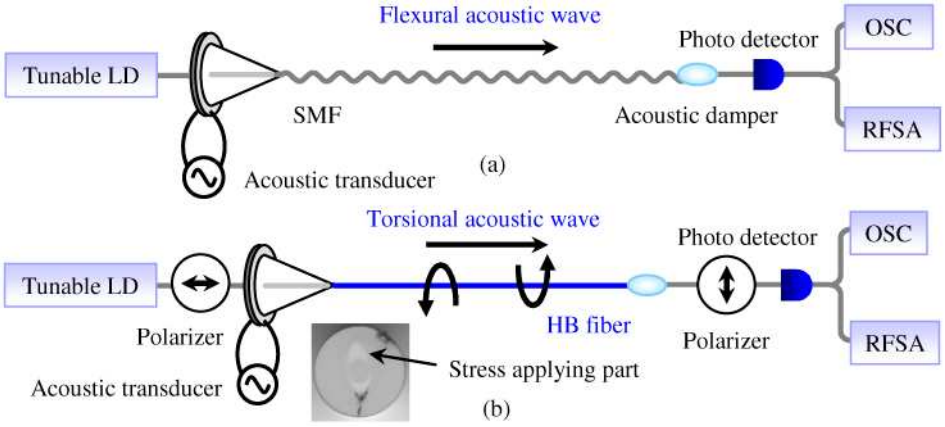

Fig. 1. Schematic of an experimental setup used to measure the time-dependent intensity modulation in (a) the all-fiber flexural mode AOTF, and (b) the all-fiber torsional mode AOTF. OSC and RFSA denote an oscilloscope and a RF spectrum analyzer, respectively. The inset of Fig. 2(b) shows the cross-section of the HB fiber with elliptical stress member used in this experiment.

Figure 2 shows the measured transmission spectra of the all-fiber flexural mode AOTF [Fig. 2(a)] and torsional mode AOTF [Fig. 2(b)] when the acoustic interaction lengths were 20 cm and 50 cm, respectively. A broadband amplified spontaneous emission (ASE) from an Erbium doped fiber amplifier (EDFA) was used as an incoherent and unpolarized light source, and the output filter spectra were monitored at the optical spectrum analyzer (OSA). The resonant center wavelengths of each filter were 1577.1 nm and 1548.6 nm at the applied acoustic frequency of 1.89 MHz and 1.332 MHz, respectively. For clear modulation contrast, the RF drive powers applied to each filter were controlled to produce 10-dB notch depth and 3-dB bandpass peak, respectively.

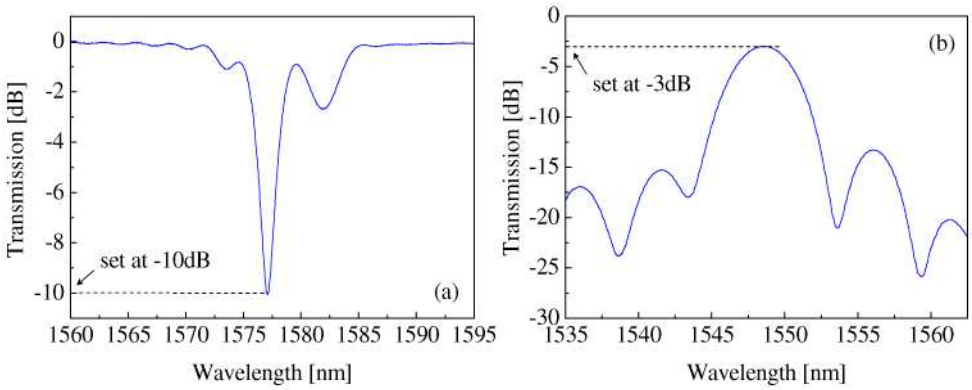

Fig. 2. Measured transmission spectra of (a) the all-fiber flexural mode AOTF at the applied frequency of 1.89 MHz, and (b) the all-fiber torsional mode AOTF at the applied acoustic frequency of 1.332 MHz. A broadband ASE source was used as an incoherent and unpolarized light source, and the output filter spectra were monitored at the optical spectrum analyzer (OSA).

The time-dependent intensity modulation of output filter signal is caused by the two factors: (1) static coupling between interacting optical modes in the fiber and (2) back reflection of applied acoustic wave, as illustrated in Fig. 3(a). Figure 3(b) shows the *f-β* diagram to illustrate the mechanism for the intensity modulation. Here, the first and the

#120153 - $15.00 USD Received 18 Nov 2009; revised 30 Jan 2010; accepted 2 Feb 2010; published 16 Feb 2010

second modes correspond to either two orthogonal polarization modes (for the torsional mode AOTF) or LP_{01} and LP_{11} modes (for the flexural mode AOTF), respectively. The input light is supposed to be in the 1st mode (LP_{01} or horizontal-polarization modes) and includes no power in the 2nd mode (the counterpart modes). However, it is not true in practice due to imperfect polarizers, nonzero stress or micro-bending induced by an adhesive at the horn tip, an acoustic damper, or fiber clamps. In contrast to the AO coupling, these kinds of static coupling do not accompany any frequency shift as illustrated by a blue arrow in Fig. 3(b). Here we assumed that the static coupling occurs prior to the AO coupling. Multiple static coupling at various locations in the device can be approximated to a single effective coupling for a given optical wavelength. The effective coupling amplitude in the 2nd mode can be described by,

$$s_{eff} = s_1 e^{i\theta_1} + s_2 e^{i\theta_2} + s_3 e^{i\theta_3} + \cdots \quad (1)$$

where, s_i and θ_i are the small amplitudes and the corresponding modal phase delays at each coupling point in Fig. 3(a), respectively.

In the AO coupling, the optical frequency of coupled mode is up- or down-shifted by an amount of applied acoustic frequency (f_a) as illustrated in Fig. 3(b) [16]. The coupling assisted by forward and backward waves has opposite slope in the f-β diagram, as denoted by red solid and dotted lines, respectively. Coexistence of the forward and backward waves generates various spots in the diagram with frequency difference by amount of f_a, the applied acoustic frequency. When one of the two modes is removed at the output, the transmitted signal will suffer from intensity modulation since it contains multiple frequency components.

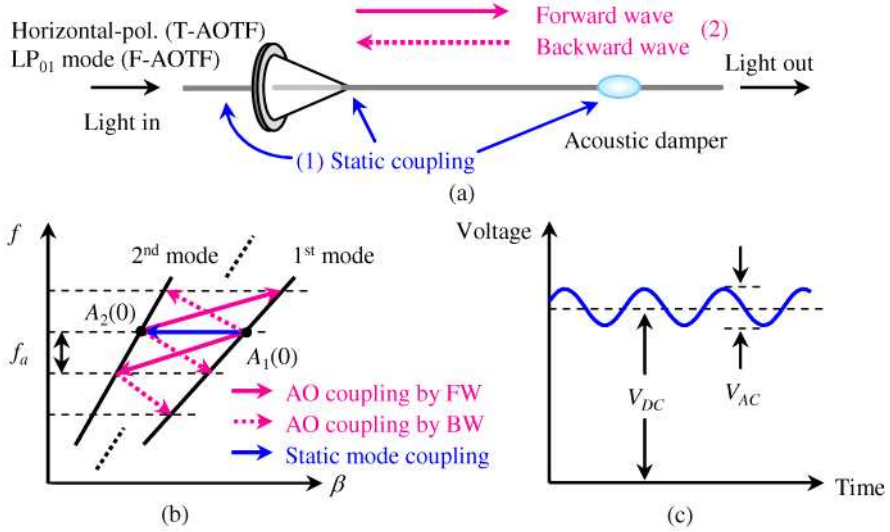

Fig. 3. (a) Two origins of the time-dependent intensity modulation of output filter signal: (1) static coupling between interacting optical modes in the fiber and (2) back reflection of applied acoustic wave. F- and T-AOTF denote the flexural and the torsional mode AOTF, respectively. (b) AO and static mode coupling between two interacting optical modes. The 1st and the 2nd modes correspond to either two orthogonal polarization modes (for the T-AOTF) or LP_{01} and LP_{11} modes (for the F-AOTF), respectively. FW and BW denote the forward and the backward acoustic waves, respectively. (c) Example of output filter signal at the resonant wavelength suffering from intensity modulation.

When the acoustic reflection is present, the coupled mode equations describing the coupling between two optical modes in the fiber can be expressed as follows [15].

$$\frac{dA_1(z)}{dz} = -i\kappa(e^{i\omega_a t} + re^{-i\omega_a t + i2KL})A_2(z)e^{i(\beta_1 - \beta_2 - K)z}, \quad (2)$$

#120153 - $15.00 USD Received 18 Nov 2009; revised 30 Jan 2010; accepted 2 Feb 2010; published 16 Feb 2010

$$\frac{dA_2(z)}{dz} = -i\kappa(e^{-i\omega_a t} + re^{i\omega_a t - i2KL})A_1(z)e^{-i(\beta_1-\beta_2-K)z}. \quad (3)$$

Here, r, κ, K, and L denote the acoustic reflection coefficient, the coupling coefficient between two modes, the propagation constant of acoustic wave, and the AO interaction length, respectively. Each A and β also denotes the normalized complex electric fields and the wave numbers of two interacting optical modes, respectively. The angular acoustic frequency, ω_a, is defined by $2\pi f_a$. When the 1st mode is coupled to the 2nd mode at the resonant wavelength, the phase matching condition $\beta_1 - \beta_2 - K = 0$ is satisfied in Eq. (2) and (3). In this case, the initial field amplitudes of each mode can be given by $A_1(0) = 1$ and $A_2(0) = s$ (<< 1), respectively. Here, s is the effective amplitude of the 2nd mode produced by the static mode coupling. From the solution of the coupled mode equations, the optical powers in the 1st mode and the 2nd mode are expressed as follows.

$$P_1(t) = |A_1(L)|^2 = \cos^2\left[\kappa L(1+r\cos\theta)\right] + s\frac{\sin\left[2\kappa L(1+r\cos\theta)\right]\sin\omega_a t}{1+2r\cos\theta}, \quad (4)$$

$$P_2(t) = |A_2(L)|^2 = \sin^2\left[\kappa L(1+r\cos\theta)\right] - s\frac{\sin\left[2\kappa L(1+r\cos\theta)\right]\sin\omega_a t}{1+2r\cos\theta}. \quad (5)$$

Here, θ is defined by $2\omega_a t - 2KL$ and small acoustic reflection (r << 1) is assumed, so that the quadratic and higher order terms of r and s can be reasonably neglected. Now $P_1(t)$ and $P_2(t)$ correspond to the output powers of notch-type flexural mode AOTF and bandpass-type torsional mode AOTF, respectively. The first terms in Eq. (4) and (5) can account for power fluctuation due to the acoustic back reflection effect, which can be rewritten by using Jacobi-Anger expansion as follows:

$$\cos^2\left[\kappa L(1+r\cos\theta)\right] = \frac{1}{2}\left[1+\cos(2\kappa L)\left(J_0(2\kappa Lr) + 2\sum_{n=1}^{\infty}(-1)^n J_{2n}(2\kappa Lr)\cos(2n\theta)\right)\right. \quad (6)$$
$$\left. -\sin(2\kappa L)\left(-2\sum_{n=1}^{\infty}(-1)^n J_{2n-1}(2\kappa Lr)\cos[(2n-1)\theta]\right)\right],$$

$$\sin^2\left[\kappa L(1+r\cos\theta)\right] = \frac{1}{2}\left[1-\cos(2\kappa L)\left(J_0(2\kappa Lr) + 2\sum_{n=1}^{\infty}(-1)^n J_{2n}(2\kappa Lr)\cos(2n\theta)\right)\right. \quad (7)$$
$$\left. +\sin(2\kappa L)\left(-2\sum_{n=1}^{\infty}(-1)^n J_{2n-1}(2\kappa Lr)\cos[(2n-1)\theta]\right)\right].$$

The temporal oscillation frequencies in each term of Eq. (6) or (7) are given by $4n\omega_a$ and $2(2n-1)\omega_a$, and they can be rewritten as $2n'\omega_a$. Therefore, when the acoustic back reflection is present in the AOTFs, output filter signal at the resonant wavelength oscillates with the even-order harmonics of the applied acoustic frequency. The second terms in Eq. (4) and (5) correspond to the interference between two kinds of intensity modulation effects caused by the static mode coupling and the acoustic back reflection. If the acoustic reflection does not exist (r = 0), the oscillation frequency is given by ω_a, which indicates that modulation frequency caused by the static mode coupling is equal to the applied acoustic frequency as discussed in Fig. 3(b). In case that both the static coupling and the acoustic reflection are present, the oscillation frequencies of the second term of Eq. (4) and (5) are expressed as $(2n' + 1)\omega_a$ by the Jacobi-Anger expansion, which means the interference between the static mode coupling and the acoustic back reflection effects gives rise to the modulation with the odd-order harmonics of applied acoustic frequency. Therefore, if both the static mode coupling and the acoustic back reflection are present, the intensity of filter output is expected to be modulated with both even- and odd-order harmonics of applied acoustic frequency.

In order to measure the modulation amplitudes of each output optical power at the resonant wavelengths, we replaced the ASE source with the fiber-coupled tunable laser diode

#120153 - $15.00 USD Received 18 Nov 2009; revised 30 Jan 2010; accepted 2 Feb 2010; published 16 Feb 2010

(LD) as shown in Fig. 1, and set the output wavelength of the LD at 1577.1 nm (for the flexural mode AOTF) and 1548.6 nm (for the torsional mode AOTF), respectively. The optical powers passed through the AOTFs are measured at a photo detector, and their temporal variations and oscillation frequencies are monitored at an oscilloscope and a RF spectrum analyzer (RFSA), respectively. Figure 4 shows the measured RF spectra and the time-varying oscillations of output filter signals for two types of all-fiber AOTFs. As can be seen in Fig. 4(b) and (d), output optical powers at the resonant peaks show time-dependent modulation phenomena. The modulation depth is defined in Fig. 3(c) by the ratio of peak-to-peak AC voltage amplitude (V_{AC}) to DC voltage (V_{DC}), and the resultant power fluctuation at the resonant peaks can be expressed as $(V_{AC}/V_{DC})^2$. The V_{DC} values were measured to 0.38 V and 1.75 V for the flexural and the torsional mode AOTFs, respectively. The measured values of each V_{AC} and corresponding power fluctuations are listed in Table 1. In the results shown in Fig. 4, a softly cured UV epoxy drop was used as an acoustic damper. The resultant power fluctuation depends on both the damper material and its geometry because they affect not only the acoustic reflection property (r) but also the static coupling strength (s). Especially, in case of the torsional mode AOTF, variation of the damper condition can increase the initial power (or amplitude s) in the 2nd mode, resulting in higher level of power fluctuations at the resonant wavelength. As an example, we measured the power fluctuation for the cases of sticky tape and fiber jacket dampers, and the related results are also summarized in Table 1. The modulation frequencies caused by the static mode coupling (f_a) and the acoustic back reflection ($2f_a$, $4f_a$, and $6f_a$) are clearly observed in Fig. 4(a) and (c) as expected in the previous section. The odd-order harmonics of applied frequency, $3f_a$ are also observed in each RF spectra, which correspond to the interference between two kinds of modulation effects as discussed above. We could observe also the same phenomena for the cases of the sticky tape and the fiber jacket dampers.

Table 1. The AC voltage amplitudes and the corresponding power fluctuations for several damper materials.

	Flexural mode AOTF		Torsional mode AOTF	
Damper material	V_{AC} [V]	$(V_{AC}/V_{DC})^2$	V_{AC} [V]	$(V_{AC}/V_{DC})^2$
Softly cured UV epoxy	0.280	54.3%	0.160	0.84%
Sticky tape	0.078	4.21%	1.100	39.5%
Fiber jacket	0.080	4.43%	0.950	29.5%

Contributions of the two origins to intensity modulation can be quantitatively estimated from the measured modulation powers by the following approach. For the small acoustic back reflection ($r << 1$) and static mode coupling ($s << 1$), Eq. (4) and (5) can be rewritten by multivariate Taylor series expansion with respect to r and s as follows.

$$P_1(t) = \sin^2(\kappa L) - s\sin(2\kappa L)\sin\omega_a t + \sin(2\kappa L)\kappa L r\cos(2\omega_a t - 2KL) + \cdots, \quad (8)$$

$$P_2(t) = \cos^2(\kappa L) + s\sin(2\kappa L)\sin\omega_a t - \sin(2\kappa L)\kappa L r\cos(2\omega_a t - 2KL) + \cdots. \quad (9)$$

Note that the amplitudes of the 1st and the 2nd harmonics are proportional to s and r, respectively. They also largely depend on the coupling efficiency (κL) of the device. The non-oscillating terms in Eq. (8) and (9) are given by,

$$\sin^2(\kappa L) = 0.1 \text{ (10-dB notch depth for the flexural mode AOTF)}, \quad (10)$$

$$\cos^2(\kappa L) = 0.5 \text{ (3-dB bandpass peak for the torsional mode AOTF)}, \quad (11)$$

and therefore, the modulation powers at f_a and $2f_a$ are also given by $0.6s$ and $0.193r$ for the flexural mode AOTF, and s and $(\pi/4)r$ for the torsional mode AOTF, respectively. Then, from the measured modulation powers at each frequency, s and r values are estimated by 7.32 ×

#120153 - $15.00 USD Received 18 Nov 2009; revised 30 Jan 2010; accepted 2 Feb 2010; published 16 Feb 2010

10^{-5} and 0.14 for the flexural mode AOTF, and 4.65×10^{-4} and 2.36×10^{-3} for the torsional mode AOTF, respectively. The results show that even those small values for acoustic reflection or static coupling can give rise to large intensity modulation in the output filter signal.

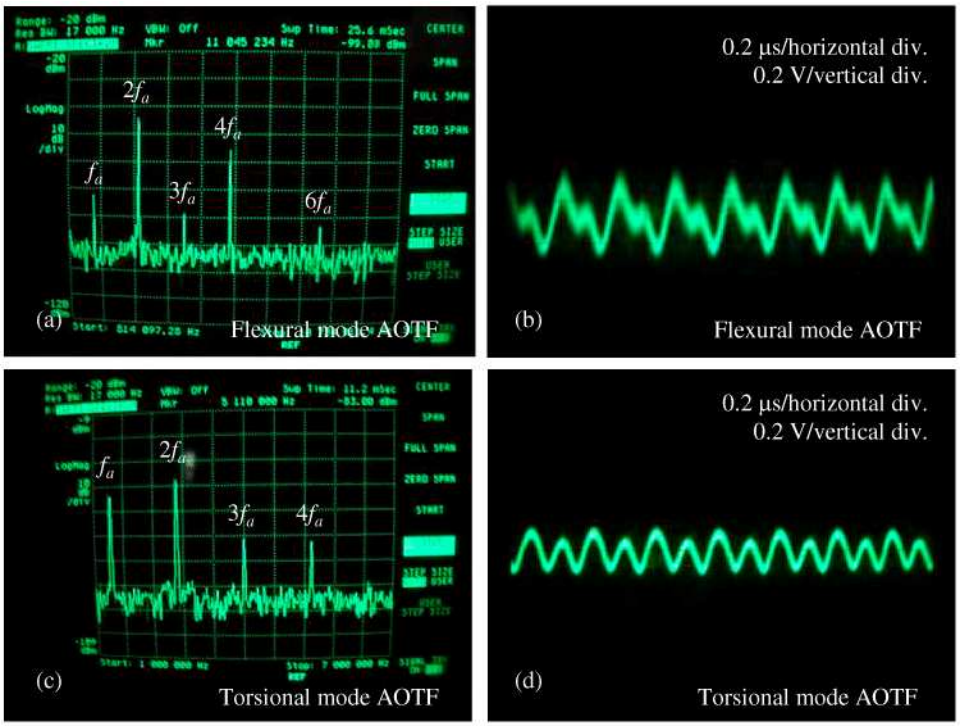

Fig. 4. Time-dependent intensity modulations in two types of all-fiber AOTFs. (a) and (c) show the measured RF spectra for the flexural mode AOTF and the torsional mode AOTF, respectively. (b) and (d) show temporal variations of output optical power at the resonant peaks measured at an oscilloscope.

Suppression of the static mode coupling at the input can be an important issue especially in case of the torsional mode AOTF due to a limited extinction ratio of the polarizers. To suppress the power fluctuation at the 1st harmonic modulation below 1% at 3-dB transmission, a polarization extinction ratio of −20dB is required. In case of the flexural mode AOTF using a cladding mode as the 2nd mode, the polymer coating on the fiber itself serves as a good mode stripper. Another important source of the static coupling is anisotropic stress or micro-bending which is often created by adhesive at the fiber-horn bonding, since they produce coupling between the two polarizations or the two spatial modes. Therefore a proper adhesive and its curing method which do not induce the stress on the fiber are required to reduce the static mode coupling.

In order to suppress the 2nd and the higher-order harmonic modulations, a proper selection of damper material and the design of its geometry are required to minimize the acoustic back reflection. The lower acoustic reflection in the torsional mode AOTF explains that the acoustic impedance matching was well achieved in our experiment. The detailed study for the optimal damper with minimal acoustic reflection is underway.

3. Conclusion

In conclusion, we have theoretically and experimentally analyzed the time-dependent intensity modulation phenomena in two types of all-fiber AOTFs utilizing the flexural and torsional acoustic waves, respectively. Output filter signals at the resonant peaks showed the

#120153 - $15.00 USD Received 18 Nov 2009; revised 30 Jan 2010; accepted 2 Feb 2010; published 16 Feb 2010

time-varying oscillations with even- and odd-order harmonics of applied acoustic frequency, which could be successfully explained by the static mode coupling and the acoustic back reflection. Contributions of the two factors to the intensity modulation could be estimated from the measured modulation powers at each frequency by our theoretical model. The design issues of the all-fiber AOTFs for suppression of unintentional intensity modulation were discussed.

Acknowledgements

We thank S. H. Yun, H. S. Kim, K. I. Lee, H. Y. Lee, and W. Sorin for valuable discussions during the early stage of the all-fiber AOTF development. This work was supported by the Regional Research Center for Photonic Materials and Devices, Chonnam National University, and the Korea Research Foundation Grant funded by the Korean Government (MOEHRD, Basic Research Promotion Fund) (KRF-2008-331-C00115).

#120153 - $15.00 USD Received 18 Nov 2009; revised 30 Jan 2010; accepted 2 Feb 2010; published 16 Feb 2010